RSC Advances

ROYAL SOCIETY OF CHEMISTRY

www.rsc.org/advances

Fabrication of Super Tough Poly(lactic acid)/Ethylene-*co*-vinyl-acetate Blends via Melt Recirculation Approach: Static-short term Mechanical and Morphological Interpretation

Rajendra Kumar, Saurindra N. Maiti[*], Anup K. Ghosh

Centre for Polymer Science and Engineering, Indian Institute of Technology Delhi,

Hauz Khas, New Delhi-110016, India

*Email address: maitisn49@yahoo.co.in

Tel.: +91-11-26591494; Fax: +91-11-26591421

Abstract: Mechanical properties such as tensile strength, tensile modulus, elongation-at-break and impact strength of poly(lactic acid) (PLA)/ethylene-*co*-vinyl-acetate copolymer (EVA, vinyl acetate content 50 weight percent) blends were evaluated at EVA volume fractions ranging from 0-0.35. Tensile properties were compared with several theoretical models. The blends lost little of the tensile strength and modulus while simultaneously enhanced elongation-at-break. Efficient dispersion of EVA in PLA using micro compounder in which there is provision of melt recirculation significantly improved Izod impact strength making blends super tough. The phase miscibility, two phase morphology, fibrillation and interparticle distance were studied by scanning electron microscopy (SEM). The blend is a two phase system where the particle size enhances upon increase in the concentration of the blending copolymer. The normalized values of relative elongation-at-break and Izod impact strength enhanced significantly in accordance with crystallinity (33 times (53.73 kJ/mm^2) at 0.35 volume fraction of EVA, which indicated softening of the system with enhanced toughness.

Key words: Poly(lactic acid); super-tough; mechanical properties; morphology; EVA co-polymer

1

1. INTRODUCTION

Increasing concern of environmental pollution and sustainability issues associated with petroleum based non-bio-degradable plastics motivated researchers to develop bio-degradable polymers.[1-2] Poly(lactic acid) (PLA), which degrades biologically, is derived from renewable sources and has drawn a significant extent of attention in recent years.[2-4] PLA exists in L- and D-forms which are optical isomers. PLA containing large concentrations of L- isomer is highly crystalline. However, the crystallinity and bio-degradability of PLA depend on the content of D-form isomer.[5] On the other hand, the processability of PLA is quite inferior to that of the general polyolefins. Despite numerous advantages such as high strength, high stiffness, good bio-compatibility, high transparency and excellent biodegradability,[5] PLA suffers from major disadvantages notably brittleness (low strain at break and high modulus), low heat distortion temperature (HDT, <60°C), poor impact strength and a low rate of crystallization [5-7] which limit its applicability.

In order to overcome the drawbacks of PLA various strategies have been followed, such as copolymerization, plasticization and blending with other polymers or rubbers.[8] Among all these approaches blending of PLA with soft and tough polymers is the most effective and convenient way to toughen PLA.[7, 9-10] Blending of PLA with immiscible polymers or partially miscible polymers leads to significant improvement in the impact strength of PLA without trading off the stiffness.[11] It is well known that in immiscible polymer blends a degree of compatibilization can be achieved by addition of a pre-made polymer with intermediate surface energy or by *in situ* reaction of polymers during melt blending.[12-15]

Blending of PLA with other polymers has been given keen attention by researchers and engineers.[8, 16-17] Previous studies on PLA blends are mainly focused on rheological properties and miscibility.[16] Many studies have been reported on blending of PLA to improve its performance. The blending polymers include poly(butylene succinate) (PBS),[18] polyurethane (PU),[19-21] polyethylene (PE),[12, 22-23] poly(vinyl acetate) (PVAc),[24-25] poly(methyl methacrylate) (PMMA),[26] poly(3-hydroxybutyrate) (PHB),[27] polycaprolactone (PCL),[28] poly(butylene adipate-*co*-terephthalate) (PBAT),[13] acrylonitrile-butadiene-styrene (ABS),[29] glycidyl methacrylate (GMA),[30] poly(ethylene-*co*-octene) (TPO),[31] and poly(*β*-hydroxybutyrate-*co*-*β*-hydroxyvalerate) (PHBV).[13] Most of these blends are immiscible resulting complete phase separation showing

limited improvement on the toughness. However, some systems are reported to have miscibility or partial miscibility, for example blends of PLA with PMMA and PVAc.

It has been shown that PLA is miscible with PVAc.[24-25] The copolymer EVA contains vinyl acetate monomer. Thus the interaction between PLA and EVA may depend on the variation of VA content in the later. Therefore the compatibility between PLA and EVA can be achieved by tuning the VA content without the need of additional compatibilizer. Ma et al.[6] reported that maximum toughness of PLA was achieved when vinyl acetate content in EVA was maintained between 50 to 60 wt. (%). Moreover, in this range, the compatibility between PLA and EVA is such that sufficient phase separation is achieved with moderate phase adhesion required for effective rubber toughening.

In this work, attempt has been made to prepare super tough PLA and to broadly study the effect of flexibility of EVA containing 50 wt. (%) of VA on the mechanical properties of PLA. To understand the phase interaction between PLA and EVA, tensile data have been analyzed employing predictive models. In order to evaluate the state of dispersion of the elastomer EVA in the matrix SEM studies have been undertaken. The notched Izod impact behaviour has been correlated with blend morphology.

2. EXPERIMENTAL

2.1. Materials

Injection moulding grade of PLA {(Ingeo 3052 D, D-isomer content = 4.2 %, melt flow index 14 g/10 min, density =1.24 g/cm^3 (210 °C and 2.16 kg load)} was purchased from NatureWorks LLC [7], USA. EVA copolymer (VA content 50 wt. %, Density 1 g/cm^3, Tg -29 °C) was procured from Lanxess Pvt. Ltd., Germany.

2.2. Blend Preparation

Both PLA and EVA copolymers were vacuum-dried at 50 °C for 12h before use. Binary blends of PLA/EVA at varying concentrations of EVA of 0-30 wt. % (Volume fraction of EVA Φ_d=0-0.35) were melt blended on a co-rotating micro extruder Haake Minijet Lab at a screw rpm 100. The processing temperature was maintained at 190 °C. The volume fraction Φ_d of the blending polymer was calculated according to Eq. (1):[32]

$$\Phi_d = (W_1/\rho_1)/[(W_1/\rho_1) + (W_2/\rho_2)] \qquad (1)$$

where W is the weight fractions and ρ the density (g/cm^3) of the constituents. Subscripts 1 and 2 denote the dispersed and the continuous phase, respectively. The PLA granules were also extruded under same conditions to ensure identical shear and thermal history as that of the blends. The details of the blend formulations and the corresponding Φ_d values are presented in Table 1.

2.3. Preparation of Test Specimens

The specimens for the evaluation of mechanical properties were micro injection molded on Haake Minijet-II micro injection molding machine. The barrel temperature was 200 °C. Injection pressure and mold temperature were 650 bar and 65 °C, respectively.

2.3.1. Mechanical Testing

Tensile tests of dumb-bell shaped specimens were performed on a Zwick universal tester, Model Z010 (Germany), at a cross-head speed 10 mm/min and cross-head separation 15 mm according to ASTM D 638 (Type 5) test procedure.[33] Izod impact strength was measured using notched specimens on a falling hammer type instrument, Model 504 plastic Impact (USA). A notch of 2 mm depth with an angle of 45° was made on the impact specimens following ASTM D256 specifications.[32] At least five samples at each composition were tested and the average values are reported. All the tests were performed at ambient temperature 30± 2 °C.

2.3.2. Differential Scanning Calorimetry (DSC)

Crystallization behaviour of PLA and that in the blends was studied by DSC on a TA Instrument, Model Q 200, in an atmosphere of liquid nitrogen. Samples were powder/flakes scraped from the injection molded tensile specimens and vacuum dried at 80 °C for 4 h. The samples were first heated from 30 °C to 200 °C at a heating rate of 5 °C/min and detained at 200 °C for 5 min to eradicate the effect of the previous thermal history. The melt is then cooled to 30 °C and again heated to 200 °C at 5 °C/min cooling and heating rates respectively. Heat of fusion values (ΔH) were employed to evaluate the crystallinity (%) of PLA in the blends using Eq. (2):

$$\text{Degree of crystallinity, } \chi, (\%) = \left[(\Delta H_m / \Delta H_\circ)/W \right] \times 100 \tag{2}$$

where, ΔH_m is the enthalpy of the fusion of PLA in the blends, ΔH_o the enthalpy of fusion of the 100 (%) crystalline PLA, 93 J/g,[16] and W the weight fraction of PLA in the sample.

2.3.3. Scanning Electron Microscopy (SEM)

The phase morphology of the impact fractured samples were observed on a scanning electron microscope, Model EVO 50, at 20 kV to evaluate the dispersion of the discrete phase in PLA. Before scanning, sample surfaces were sputter coated with a thin layer of silver. The SEM micrographs were analyzed using image analysis software, Image J, to calculate the diameter of the dispersed phase. The weight average particle size, d_w of EVA was calculated from a mean of minimum 200 particles using Eq. (3):[34]

$$d_w = \sum n_i d_i^2 / \sum n_i d_i \qquad (3)$$

where n is the number of particles with diameter d. The interparticle spacing, i.e. the ligament thickness, τ was determined from d_w and Φ_d following Eq. (4):[32]

$$\tau = d_w [(\pi / 6\Phi_d)^{1/3} - 1] \qquad (4)$$

In Eq. (4), EVA particles were assumed uniform spheres arranged in a cubic lattice.

3. RESULTS AND DISCUSSION

3.1. Degree of Crystallinity

Figure 1 shows the DSC heating scans of the samples and corresponding parameters of PLA are depicted in Table 1. It is observed that presence of EVA do not influence the glass transition temperature (T_g) of PLA. From the DSC measurements, the endothermic peak temperature and peak height give information about crystal size and its size distributions. Moreover the number of peaks gives information of different crystal structure (bimodal), and normalized enthalpy gives information about degree of crystallinity.[35] For the second heating, exotherm peaks appear which is a well-known feature of PLA crystallization during DSC measurements.

Table 1. Compositions and values of DSC crystallization parameters of PLA in PLA/EVA blends

PLA (wt. %)	EVA (wt. %)	Volume Fraction (Φ_d)	T_g (°C)	T_{cc} (°C)	ΔH_{cc} (J/g)	T_m (°C)	ΔH_m (J/g)	X_c (%)
100	0	0	60.9	104.8	31.1	154.9	29.3	32
95	5	0.06	61.1	125.8	24.7	151.6	27.0	31
90	10	0.12	61.2	126.8	19.2	152.1	22.9	28
80	20	0.24	61.4	125.4	18.7	151.7	20.8	27
70	30	0.35	61.9	126.4	10.3	151.3	15.2	23

The heating curve of neat PLA shows very distinct exothermic peaks and double melting peaks for cold crystallization temperature (T_{cc}) and melting temperature (T_m) respectively. With the increase of EVA concentration the cold crystallization peak weakens and significantly shifted to higher temperatures which indicate that the cold crystallization of PLA becomes more difficult and less PLA can transform into crystalline state. This can be explained on the basis that during heating process EVA melts prior to PLA and possibly promotes the chain mobility in the interface of PLA and EVA subsequently playing plasticizing role in promoting the cold crystallization of PLA.[16] Consequently crystallinity (%) of PLA decreases with increase of EVA wt. (%). However, the decrease in the crystallinity of PLA may be due to the physical presence of increasing concentration of EVA which disrupts the continuity of the PLA matrix. Moreover, this is possibly due to the enhanced phase adhesion between PLA and EVA, which prevents the migration of PLA chain segments out from the EVA phase, hence limits the crystallization of PLA.[10, 16]
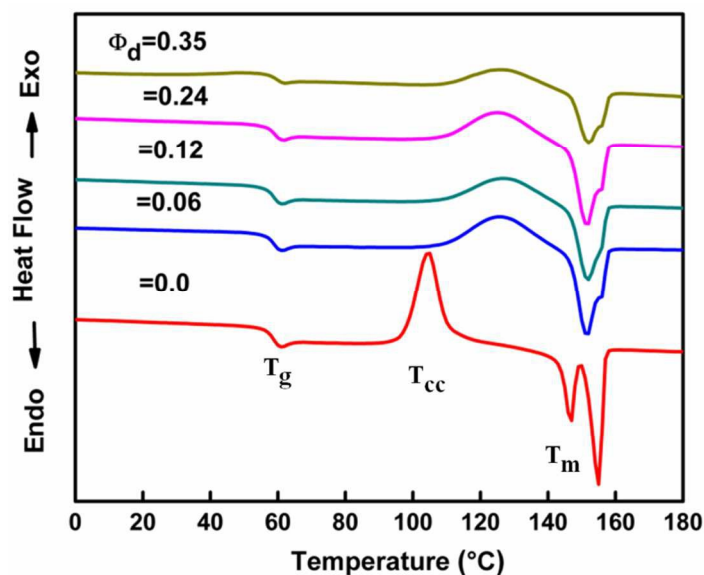

Figure 1: DSC traces of PLA and PLA/EVA blends recorded during the second heating at 5 °C/min.

Since the crystallinity plays an important role in the properties of PLA/EVA blends, this parameter will be considered in the subsequent sections in the analysis of the mechanical properties.

3.2. Mechanical Properties

3.2.1. Tensile Stress-strain Curves

Tensile stress-strain curves of PLA and PLA/EVA blends are shown in Figure 2. Neat PLA fails once it passes the yield point. The stress-strain curve of EVA is that of a typical rubbery polymer without distinct yield point up to 1300% elongation-at-break, Figure 2, inset. Neat PLA possesses strong strain softening which is not stabilized by a strain hardening during breaking, subsequently strain softening initiates strain localization causing local tri-axial stress concentration.[8] Because of the absence of local strain delocalization, local tri-axial stresses induce void nucleation and crazes leading to brittle failure behaviour of PLA.[8] Incorporation of EVA in PLA causes lower yield stress with broadening of yield peak because of release of tri-axial stress or enhanced delocalization of strain introduced by flexible EVA copolymer.[6, 8] Elongation-at-break enhanced with Φ_d and at the maximum Φ_d the parameter was 225%. PLA/EVA blends exhibited strain softening followed by neck formation and strain hardening which indicates the ductility of the blends.
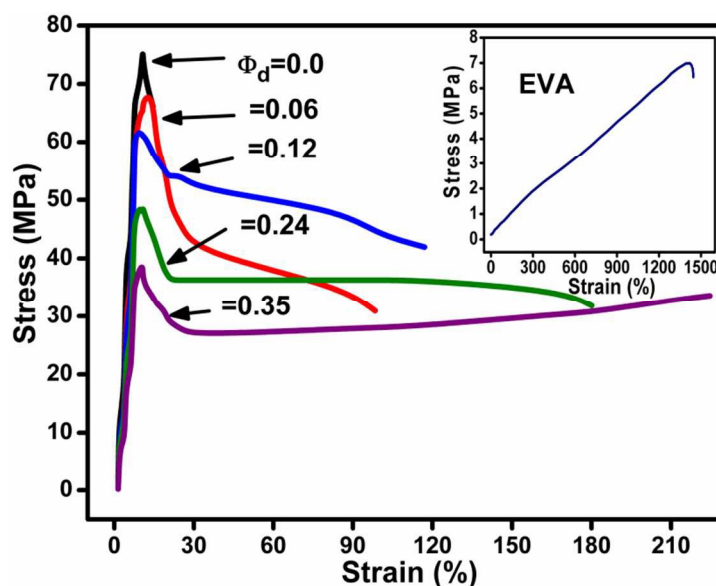

Figure 2: Variation of stress and strain with Φd in PLA/EVA blends. Inset: Variation of stress and strain for pure EVA

Table 2. Tensile property results of PLA/EVA blends

Φ_d	X_c (%)	Tensile Modulus (MPa)	Tensile Strength (MPa)	Elongation-at-break (%)
0	32	439±16.56	75±0.51	16±1.25

0.06	31	416±26.21	65±2.92	21±1.76
0.12	28	327±27.3	60±0.55	30±1.99
0.24	27	255±39.8	47±2.16	146±10.76
0.35	23	205±12.37	35±1.09	164±5.89

The yield stress lowering of PLA/EVA blends with an accompanying elongation increase than that of pure PLA may be ascribed to the stress concentration effect of rubbery EVA co-polymer. The area under the stress-strain curve of PLA increased significantly upon incorporation of EVA at the entire range of Φ_d which indicated that toughness of the blends are higher than that of PLA. This enhanced toughness is attributed to increased energy absorption and enhanced ductility brought about by the elastomer EVA as reported in other rubber modified polymers also.[32, 34, 36]

Tensile properties e.g. the tensile modulus, tensile strength and elongation-at-breaks are evaluated from the stress-strain curves and are presented in Figs. 3-5 as the ratios of the property of the blends (subscript b) to that of the neat PLA matrix (subscript m) as a function of the volume fraction, Φ_d.
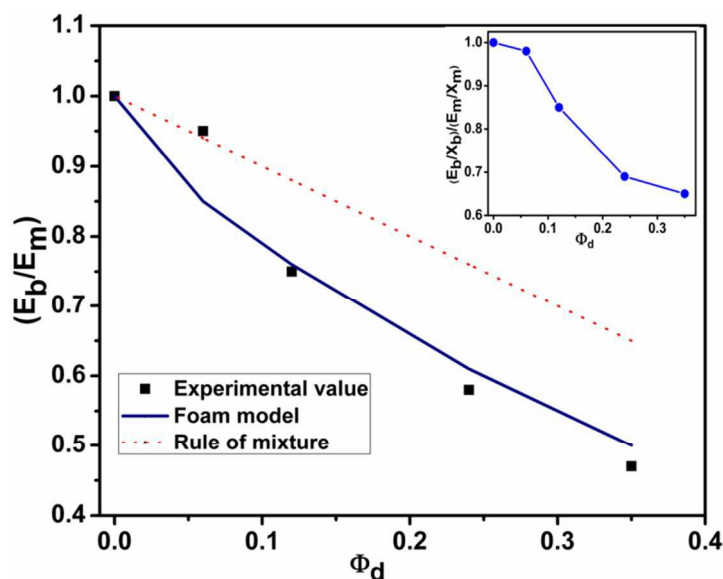
3.2.2. Tensile Modulus

Figure 3: Plot of variations of E_b/E_m of PLA/EVA blends against Φ_d and their predictive behaviour according to the foam model and rule of mixture. Inset: Dependence of normalized tensile modulus, $[(E_b/X_b)/(E_m/X_m)]$, of PLA/EVA blends against Φ_d

The tensile modulus variations with crystallinity of PLA in PLA/EVA blends are presented in Table 2. The modulus value decreases substantially with decrease in crystallinity (%) which indicates that PLA is significantly softened by the presence of flexible EVA co-polymer. The softening is caused by decrease in crystallinity as well as flexibility of EVA.

Figure 3 presents variations of the relative tensile modulus, E_b/E_m, of the PLA/EVA blends as a function of Φ_d. The relative modulus shows substantial decrease with increase in Φ_d implying that PLA is significantly softened by EVA copolymer. The blend structure was evaluated by comparing experimental data with simple theoretical predictions according to the "rule of mixture"[32, 37] Eq. (5), as well as the "foam model"[32, 34] Eq. (6):

$$(E_b / E_m) = [E_d / E_m - 1]\Phi_d + 1 \qquad (5)$$

$$(E_b / E_m) = [1 - \Phi_d^{2/3}] \qquad (6)$$

Here, E_b is the modulus of the blends, E_m the modulus of the matrix polymer PLA, and E_d the modulus value for EVA. In these calculations, the modulus values of the PLA (E_m=439 MPa) and the blends (E_b) were determined from the initial slopes of the stress vs. strain curves. The modulus value E_d of the EVA copolymer was 0.19 MPa, which was 1% secant modulus at 10 mm/min cross-head speed. In the foam model, since the modulus ratio E_d/E_m was negligible, the dispersed phase was considered a noninteracting void or pore.

The relative modulus data were in close agreement with the rule of mixture at Φ_d=0.06, however the data at higher Φ_d were lower than the theory and agreed well with the foam model, (Figure 3). It indicates that at Φ_d =0.06 some kind of phase interaction may be operative, whereas at higher concentrations the elastomeric phase may function as a diluting or flexibilizing agent.

In order to evaluate the flexibilizing effect of EVA on the matrix, the effect of crystallinity of PLA was eliminated by normalizing the relative modulus data by the crystallinity of PLA in the blends (X_b) and the matrix (X_m) respectively. Figure 3 inset, presents the plot of normalized relative tensile modulus, $[(E_b/X_b)/(E_m/X_m)]$ against Φ_d. The value decreased drastically with increase in Φ_d and at the highest Φ_d of 0.35 the decrease was 0.7 times. This indicates that the elastomer is indeed a flexibilizing dispersed phase facilitating nonspecific phase interaction with the continuous PLA phase. Similar observations were reported in PP/EVA blends too.[38]

3.2.3. Tensile Strength

The variation of tensile strength with crystallinity of PLA in PLA/EVA blends is given in Table 2. The tensile strength of PLA/EVA blends decreases continuously with decrease in crystallinity of PLA, which may be due to interference in the nucleation and growth of PLA crystals by the presence of flexible blending polymer EVA.

Table 3. Values of the stress concentration factor α, Eq. (7), and adhesion parameter K, Eq. (8), in PLA/EVA blends

Φ_d	K	α
0	-	-
0.06	0.77	2.32
0.12	0.82	1.86
0.24	0.97	1.93
0.35	1.07	2.16
Mean value	0.91	2.06

Figure 4 presents variations in the relative tensile strength (ratio of the relative tensile strength of PLA/EVA blends to that of the PLA, σ_b/σ_m) vs. Φ_d. The tensile strength of PLA continuously decreased with increasing Φ_d. This weakening of blend structure may be attributed to the softening effect of EVA copolymer which subsequently decreases the effective cross sectional area of the continuous PLA phase. Similar results were reported in other toughened polymer systems also where elastomer is the discrete phase.[32, 37] The decrease in the tensile strength is the consequence of decrease in the crystallinity, similar trend was observed in the tensile modulus also (Table 2). The relative tensile strength data were analyzed following simple predictive models, the "Porosity model" [32, 37, 39] Eq. (7), and the "Nicolais Narkis model" [34, 37, 40] Eq. (8), to evaluate the discontinuity or weakness introduced by the dispersed phase EVA:

$$\sigma_b / \sigma_m = \left[\exp(-\alpha.\Phi_d)\ \right] \tag{7}$$

$$\sigma_b / \sigma_m = \left[1 - K\Phi_d^{2/3}\ \right] \tag{8}$$

Similar models have been employed in other two phase systems of polymer blends/composites [37]. These models assume no adhesion between the two phases [37] and tensile strength depends on either the area fraction or the volume fraction of the dispersed phase i.e. $\Phi_d^{2/3}$ or Φ_d respectively. Detailed descriptions about the theories and the significance of the parameters are available

elsewhere.[39] In Eq. (8), low value of the interaction parameter K, also known as weightage factor, denotes higher phase interaction. Although K=1.21 denotes poor adhesion, K=0 describes significant adhesion so that the strength of the polymer matrix does not decrease. Similarly the value of parameter α describes stress concentration, higher the value of α higher the stress concentration.[32, 37, 41-42]
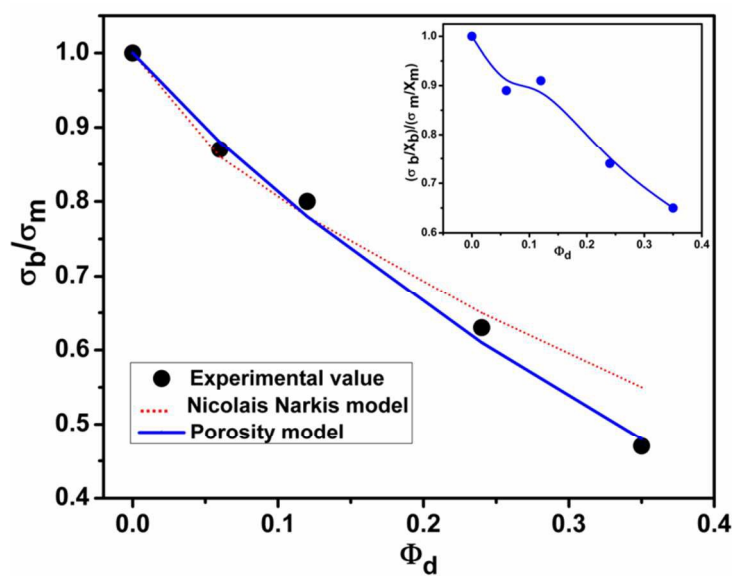

Figure 4: Plot of variations of σ_b /σ_m of PLA/EVA blends (▪), Porosity model (-), [Eq. (7)] with α=2.06, and Nicolais Narkis model (…), [Eq. (8)] with K=0.91, against Φ_d. Inset: Variations of normalized relative tensile strength [$(\sigma_b/X_b)/(\sigma_m/X_m)$] of PLA/EVA blends against Φ_d

Table 3 depicted the values of α and K for each Φ_d value obtained from comparisons of experimental tensile strength data with Eqs. (7) and (8). According to Nicolais Narkis model[40] Eq. (8), the values of K were less than one with mean value of 0.91, which denotes a good degree of adhesion and subsequently smaller extent of weakness in the blend structure.[43-44] Gupta and Purwar[45] reported similar results earlier in the PP/SEBS/HDPE and PP/SEBS/PS blends. Porosity model, Eq. (7) and Table 3, exhibit significant degree of stress concentration with the value of a=2.06. This value is almost close to the value 2.04 reported in iPP/CSM blend.[46]

The variations of normalized relative tensile strength data, $(\sigma_b/X_b)/(\sigma_m/X_m)$, against Φ_d are presented in Figure 4 inset, to evaluate the effects of phase interaction and flexibility of EVA on PLA. Here X_b and X_m represent crystallinity of PLA in PLA/EVA blends and that of neat PLA respectively. The normalized tensile strength of PLA decreased continuously on blending with EVA co-polymer (increasing Φ_d). The data were less than unity at Φ_d=0.06-0.35. This

11

weakening of the blend structure may be because of the decrease in the effective load bearing cross-sectional area of the matrix polymer in the presence of the co-polymer, similar to other elastomer-modified systems. [47] The decrease in tensile strength is also aided by the flexibility of EVA. Thus, there is no apparent phase adhesion observed, the flexibility of blending polymer predominates and consequently tensile strength decreases in the presence of EVA co-polymer.

3.2.4. Elongation-at-break

The variation of elongation-at-break with crystallinity (%) of PLA/EVA blends is presented in Table 2. The increase in elongation-at-break with decrease in crystallinity may be attributed to enhanced amorphization of PLA along with the flexibility of the blending polymer which eventually make PLA more ductile.
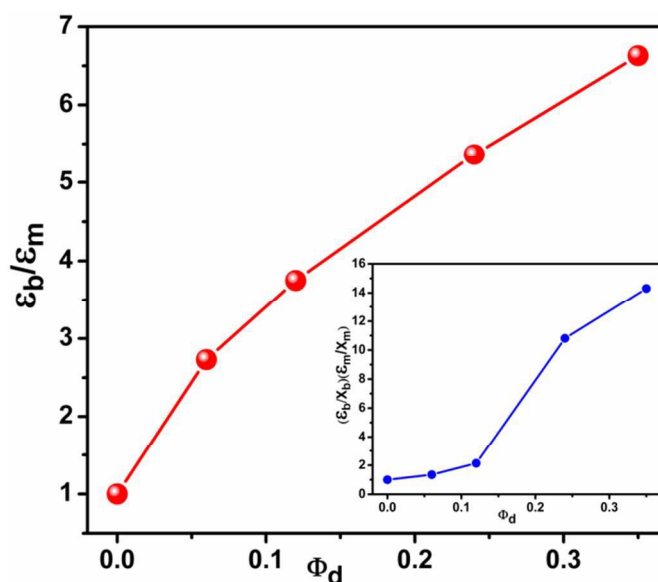

Figure 5: Variation of relative elongation-at-break ($\varepsilon_b/\varepsilon_m$) of PLA/EVA blends against Φ_d. Inset: Variation of relative normalized elongation-at-break (ε_b/X_b)/(ε_m/X_m) of PLA/EVA blends with Φ_d

Figure 5 exhibits variation of relative elongation-at-break ($\varepsilon_b/\varepsilon_m$) against Φ_d. The $\varepsilon_b/\varepsilon_m$ of PLA/EVA blends increased with Φ_d. The increase is attributed to enhanced ductility of the system due to increase in amorphization of PLA along with the flexibility of EVA. The continuous increase in the value of $\varepsilon_b/\varepsilon_m$ with Φ_d indicates significant increase in the ductility of PLA caused by the EVA copolymer.

Initially the data increase to a small extent up to $\Phi_d=0.12$; however, beyond $\Phi_d=0.12$ the increment was quite significant, at $\Phi_d=0.24$ and $\Phi_d=0.35$, the values increased by 9.13 times and 10.25 times respectively. Tensile moduli data also showed significant matrix softening in the presence of EVA copolymer.

It may be noted here that enhancement of ductility of PLA may be due to flexibility of the discrete phase and enhanced amorphization of PLA. The modulus decrease of PLA in the presence of EVA also indicated the matrix softening. The softening of PLA matrix indicates toughening of polymer under impact mode of load application. Moreover, toughened polymer will consume additional energy to break and the fracture mechanism may also change similar to a ductile material.

To examine the effect of the flexibility of EVA co-polymer on the enhancement of ductility of PLA, the effect of crystallinity of PLA was eliminated. Figure 5 inset presents relative normalized elongation-at-break, $(\varepsilon_b/X_b)/(\varepsilon_m/X_m)$, against Φ_d. The data continuously increased in the entire range of Φ_d confirming enhanced ductility due to matrix softening in presence of the elastomer phase. Initially the data increased by a small extent up to $\Phi_d=0.12$, however, beyond $\Phi_d=0.12$, the increase in the elongation was very significant.

3.2.5. Impact Strength

The notched Izod impact strength of PLA/EVA blends enhanced with the decrease in crystallinity (%) as shown in Table 4. Initially up to $\Phi_d=0.12$, the data increased to a small extent, however, beyond $\Phi_d=0.12$, sharp increase in the impact strength was observed. The notched Izod impact strength of the blends is low when EVA percent is less than 10 wt. % ($\Phi_d=0.12$) which may be due to the fact that small EVA particles are difficult to cavitate under the impact condition. The increase in the impact values with decrease in crystallinity may be due to combined effect of enhanced amorphization of PLA and flexibility of EVA.[32]

To eliminate the effect of crystallinity on the variation of impact strength, the relative Izod impact strength value of PLA/EVA blends were normalized and presented in Figure 6 against Φ_d. Initially upto $\Phi_d=0.12$, normalized impact data increased to a small extent, however, beyond $\Phi_d=0.12$, the data increased drastically. The normalized impact strength at maximum Φ_d is ~33 times that of PLA, making the blend super tough, which indicates that the elastomer EVA toughened PLA substantially.[7] This increase is related to the enhanced ductility of the blend due

to increased flexibility by EVA which creates increased extent of shear yielding. The variation of impact strength against Φ_d exhibits similar behavior with that of the elongation data implying enhanced ductility in the system.[36, 48-49]
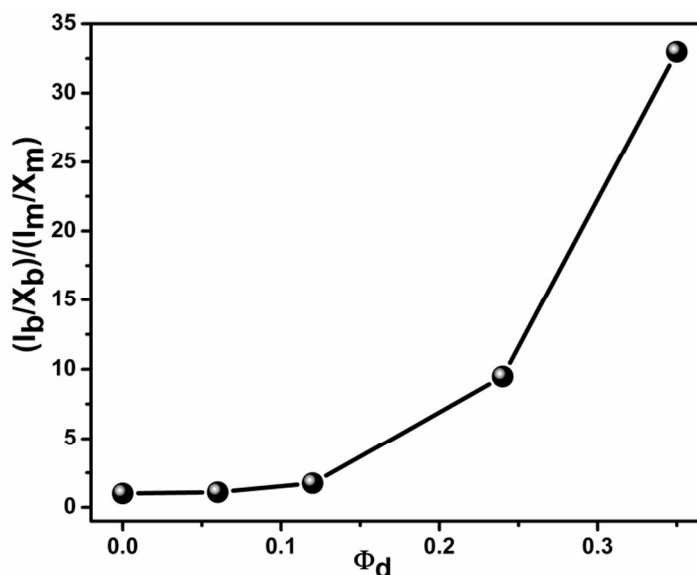

Figure 6: Variation of normalized impact strength $(I_b/X_b)/(I_m/X_m)$, of PLA/EVA blends against Φ_d

3.3. Fracture Surface Morphology and Mechanism of Toughening

The cross-section images of impact fractured surface morphology of PLA/EVA blends are shown in Figure 7 (a-e). PLA exhibits sharp ridges characteristic of a brittle fracture, (Figure 10 a), without indicating shear yielding. The blends exhibited two phase morphology e.g. sea-island morphology where EVA is the dispersed phase in the PLA matrix. Furthermore, in the sea-island morphologies EVA exhibits varying particle diameters with increase in Φ_d. At low concentration the EVA droplets are small in size and mostly spherical shaped with a small percentage of them being slightly elongated, (Figure 10 b, c). With further increase in Φ_d the droplets are mostly elongated and droplet size enhanced as well. The elongated shape of the dispersed phase with increasing Φ_d can be explained on the basis that during injection moulding process of the blends at high shear rate, the softer elastomeric phase shows elongational flow into the relatively harder PLA phase. Due to enhanced ease of deformation of the elongated elastomer particles into the neighboring stressed area, shear yield stress of the matrix decreases.[50-51]

14

Table 4. Values of impact strength (I_b), domain size (d_w), and interparticle distance (τ), of PLA/EVA blends

Φ_d	d_w (μm)	τ (μm)	I_b (J/m)
0	-	-	17.1 (2.27)
0.06	0.51	0.54	18.1 (2.34)
0.12	0.55	0.35	25.5 (3.39)
0.24	1.10	0.33	136 (18.19)
0.35	1.91	0.27	403 (53.73)

Note: Values in the parentheses indicates impact strength in kJ/m^2

The dispersed phase particle size increased with Φ_d, (Figure10 b-d), which may be attributed to the increasing dynamic coalescence,[34, 47] of the elastomer particles facilitated by the lower viscosity of PLA at processing temperature. The blends show signs of elongation and tearing of the elastomer phase over a larger area, the extent of which increases with Φ_d, (Figure 10 b-e). The images of Φ_d=0, 0.06 and 0.12 (Figure 7f) indicated the brittle failure, since complete breakage take place in these impact tested samples. Moreover sample Φ_d=0.24 and 0.35 exhibited partial breakage of impact tested sample, a indication of improved toughness and ductility, which can be result of various fracture mechanism such as crazing/micro-cracks, fibrillation, shear yielding etc.[52-53] Therefore, improved toughness and high impact strength are results from special combination of energy absorption mechanism that arrested the crack tip. Significant extent of whitening was observed in SEM micrographs of the blends which enhanced with increase in Φ_d which may be due to the yielding of the elastomer phase at the interphase region as well as in the droplets which also dissipate energy. The stress whitening at all around the fractured surfaces for Φ_d=0.24 and 0.35 illustrated plastic deformation of the matrix PLA indicating shear yielding reported in similar other works.[6, 52]
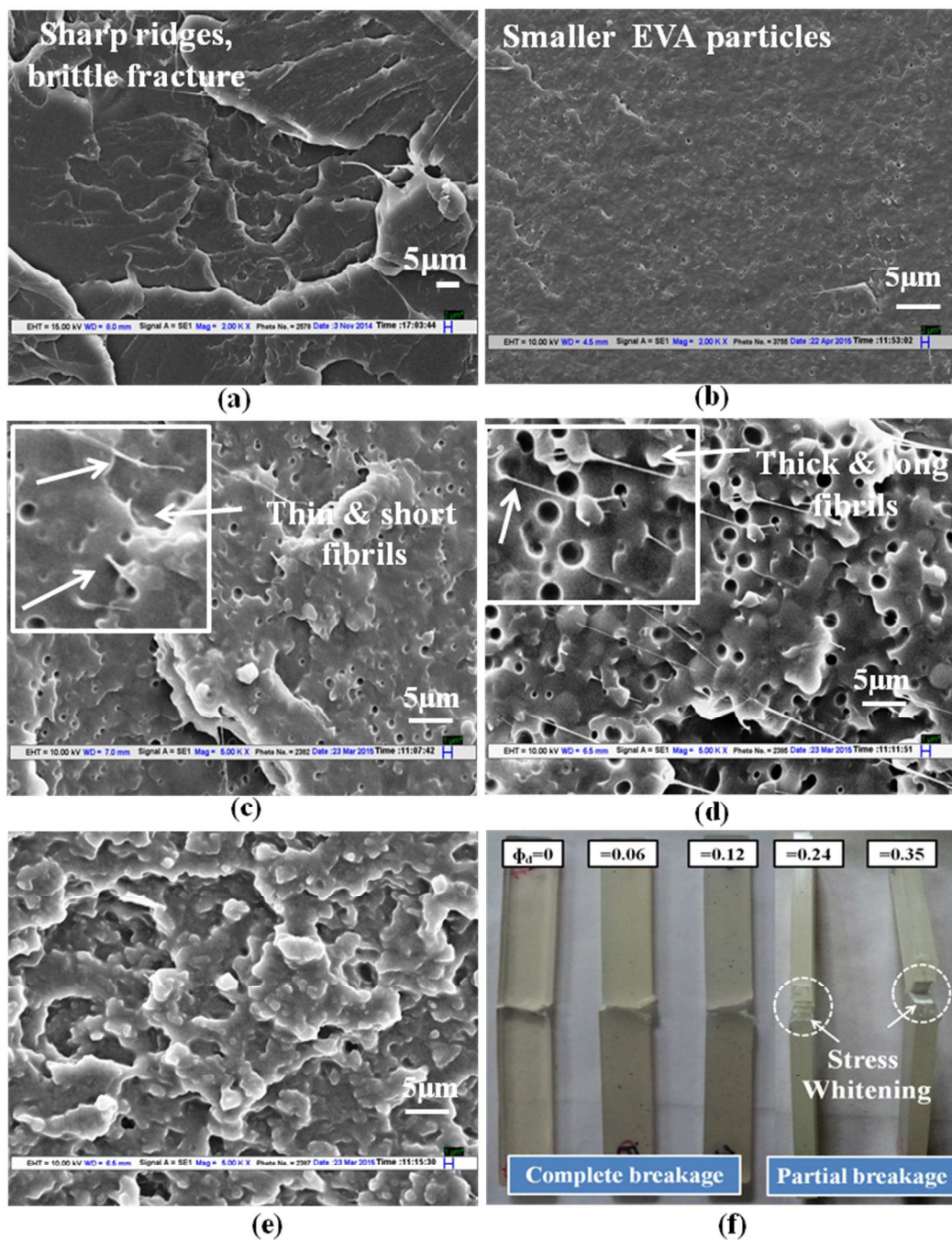
Figure 7: Scanning electron micrograph of PLA/EVA blends at 2000 magnification at varying Φ_d: (a) 0, (b) 0.06, (c) 0.12, (d) 0.24 and (e) 0.35. Figure 7 (f) contains photographs of notched Izod impact fractured samples. Samples Φ_d=0, 0.06 and 0.12, shown complete breakage while Φ_d=0.24 and Φ_d=0.35 partial breakage with extensive stress whitening.

Because of low crack initiation as well as low crack propagation energy PLA possesses low Izod impact strength.[52] Thus, the polymer is considered as brittle as in case of type-II polymer

according to Wu's definition.[37, 54] Toughening of this type of polymer blends has been shown to be due to matrix yielding introduced as a result of the elastomer's interactions with the surrounding stress field at a critical value of ligament thickness (interparticle distance, τ). The parameters τ was calculated (Table 4) from the weight average particle diameter, d_w, and volume fraction, Φ_d (Eq. 4). The τ value ranged from 0.54 μm to 0.27 μm, as Φ_d varied from 0.06 to 0.35.
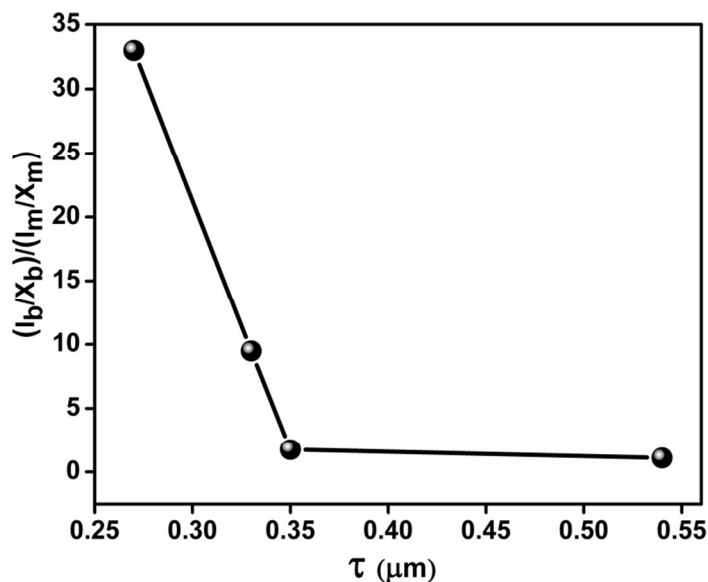

Figure 8: Variation of normalized impact strength $(I_b/X_b)/(I_m/X_m)$ of PLA/EVA blends against τ

PLA is a semicrystaline polymer and the crystallinity decreases with the increase in the EVA concentration. The crystallinity of PLA and ligament thickness, τ, will determine the impact strength of PLA/EVA blends. The variations of normalized relative impact strength $(I_b/X_b)/(I_m/X_m)$ against τ is shown in Figure 8. As shown earlier that at maximum $\Phi_d=0.35$, the normalized impact strength enhanced ~33 times (53.73 kJ/m^2) that of PLA. In the studied range of EVA concentrations, the result indicates that impact strength of the blends increases with decrease in ligament thickness, τ. At $\tau = 0.33$ and $\tau = 0.27$ the impact strength increased to ~8 times and ~33 times respectively. This increase may be due to a combination of fibrillation, crazing and extensive shear yielding caused by the EVA co-polymer. Flexibility of EVA, enhanced amorphization of PLA and creation of stress concentration may be assigned to the crazing, fibrillation and extensive shear yielding which ultimately led to the formation of super tough PLA.

4. Conclusions

Incorporation of EVA co-polymer into PLA decreases the crystallinity and substantially enhances its flexibility. The tensile modulus and strength decrease while toughness and ductility increase significantly with increase in EVA contents. The normalized tensile modulus values decreased significantly with increase in Φ_d and at the highest Φ_d of 0.35 it decreased to 0.5 times, exhibiting that the elastomer is indeed a flexibilizing dispersed phase facilitating nonspecific phase interaction with the continuous PLA phase. The normalized tensile strength of PLA decreases continuously on blending with EVA co-polymer (increasing Φ_d), indicating decrease in the effective load bearing cross-sectional area of the matrix polymer. Normalized relative notched Izod impact strength enhanced with increasing Φ_d, at maximum $\Phi_d=0.35$, the value enhanced ~33 times (53.73 kJ/mm^2) making the blend super tough. A two-phase morphology is noticed by the SEM analysis where the elastomer exists as the dispersed phase. Spherical shaped EVA particles are uniformly dispersed in the PLA matrix. The droplets become elongated and the size increased at higher EVA contents. Shear yielding of elastomer in elastomer phase as well as at PLA-EVA inter-phase led to stress whitening.

5. Acknowledgments

RSC Advances Accepted Manuscript

6. References

1. B. Eling, S. Gogolewski and A. Pennings, *Polymer*, 1982, **23**, 1587-1593.

2. R. M. Rasal, A. V. Janorkar and D. E. Hirt, *Progress in Polymer Science*, 2009, **35**, 338-356.

3. J.-S. Yoon, S.-H. Oh, M.-N. Kim, I.-J. Chin and Y.-H. Kim, *Polymer*, 1999, **40**, 2303-2312.

4. M.-J. Liu, S.-C. Chen, K.-K. Yang and Y.-Z. Wang, *RSC Advances*, 2015, **5**, 42162-42173.

5. D. Van Cong, T. Hoang, N. V. Giang, N. T. Ha, T. D. Lam and M. Sumita, *Materials Science and Engineering: C*, 2011, **32**, 558-563.

6. P. Ma, A. B. Spoelstra, P. Schmit and P. J. Lemstra, *European Polymer Journal*, 2013, **49**, 1523-1531.

7. K. Hashima, S. Nishitsuji and T. Inoue, *Polymer*, 2010, **51**, 3934-3939.

8. P. Ma, D. G. Hristova-Bogaerds, J. G. P. Goossens, A. B. Spoelstra, Y. Zhang and P. J. Lemstra, *European Polymer Journal*, 2011, **48**, 146-154.

9. E. Fortunati, D. Puglia, J. M. Kenny, M. M.-U. Haque and M. Pracella, *Polymer Degradation and Stability*, 2013, **98**, 2742-2751.

10. Y. Shi, Y. Li, J. Wu, T. Huang, C. Chen, Y. Peng and Y. Wang, *Journal of Polymer Science Part B: Polymer Physics*, 2011, **49**, 267-276.

11. V. Ojijo and S. S. Ray, *Polymer*, 2015, **80**, 1-17.

12. H. T. Oyama, *Polymer*, 2009, **50**, 747-751.

13. P. Ma, X. Cai, Y. Zhang, S. Wang, W. Dong, M. Chen and P. J. Lemstra, *Polymer Degradation and Stability*, 2014, **102**, 145-151.

14. J.-B. Zeng, K.-A. Li and A.-K. Du, *RSC Advances*, 2015, **5**, 32546-32565.

15. Y. Bian, C. Han, L. Han, H. Lin, H. Zhang, J. Bian and L. Dong, *RSC Advances*, 2014, **4**, 41722-41733.

16. Y. Li, L. Liu, Y. Shi, F. Xiang, T. Huang, Y. Wang and Z. Zhou, *Journal of applied polymer science*, 2010, **121**, 2688-2698.

17. R. Arjmandi, A. Hassan, S. J. Eichhorn, M. M. Haafiz, Z. Zakaria and F. A. Tanjung, *Journal of Materials Science*, 2015, **50**, 3118-3130.

18. T. Yokohara and M. Yamaguchi, *European Polymer Journal*, 2008, **44**, 677-685.

19.   G.-C. Liu, Y.-S. He, J.-B. Zeng, Y. Xu and Y.-Z. Wang, *Polymer Chemistry*, 2014, **5**, 2530-2539.

20.   H. Xiu, C. Huang, H. Bai, J. Jiang, F. Chen, H. Deng, K. Wang, Q. Zhang and Q. Fu, *Polymer*, 2014, **55**, 1593-1600.

21.   B. Imre and B. Pukanszky, *European Polymer Journal*, 2013, **49**, 1215-1233.

22.   K. S. Anderson and M. A. Hillmyer, *Polymer*, 2004, **45**, 8809-8823.

23.   H. Balakrishnan, A. Hassan, M. U. Wahit, A. A. Yussuf and S. B. A. Razak, *Materials & Design*, 2010, **31**, 3289-3298.

24.   A. M. Gajaria, V. Dave, R. A. Gross and S. P. McCarthy, *Polymer*, 1996, **37**, 437-444.

25.   J. W. Park and S. S. Im, *Polymer*, 2003, **44**, 4341-4354.

26.   J. L. Eguiburu, J. J. Iruin, M. J. Fernandez-Berridi and J. San Roman, *Polymer*, 1998, **39**, 6891-6897.

27.   M. A. Abdelwahab, A. Flynn, B.-S. Chiou, S. Imam, W. Orts and E. Chiellini, *Polymer Degradation and Stability*, 2012, **97**, 1822-1828.

28.   A. K. Mitra, R. U. Rao, K. N. S. Suman and V. Rambabu, *Procedia Materials Science*, 2014, **6**, 1266-1270.

29.   Y. Li and H. Shimizu, *European Polymer Journal*, 2009, **45**, 738-746.

30.   H. Liu, L. Guo, X. Guo and J. Zhang, *Polymer*, 2011, **53**, 272-276.

31.   C.-H. Ho, C.-H. Wang, C.-I. Lin and Y.-D. Lee, *Polymer*, 2008, **49**, 3902-3910.

32.   R. Sharma and S. N. Maiti, *Polymer-Plastics Technology and Engineering*, 2014, **53**, 229-238.

33.   P. Ma, D. G. Hristova-Bogaerds, P. Schmit, J. G. P. Goossens and P. J. Lemstra, *Polymer International*, 2012, **61**, 1284-1293.

34.   R. Sharma and S. N. Maiti, *Polymer Engineering & Science*, 2013, **53**, 2242-2253.

35.   W. Stark and M. Jaunich, *Polymer Testing*, 2011, **30**, 236-242.

36.   Z. Bartczak, A. Galeski, M. Kowalczuk, M. Sobota and R. Malinowski, *European Polymer Journal*, 2013, **49**, 3630-3641.

37.   N. Tomar and S. N. Maiti, *Journal of applied polymer science*, 2007, **104**, 1807-1817.

38.   D. Kakkar and S. N. Maiti, *Journal of applied polymer science*, 2011, **123**, 1905-1912.

39.   L. E. Nielsen, *Journal of applied polymer science*, 1966, **10**, 97-103.

40.   L. Nicolais and M. Narkis, *Polymer Engineering & Science*, 1971, **11**, 194-199.

41.   C. Simoes, J. Viana and A. Cunha, *Journal of applied polymer science*, 2009, **112**, 345-352.

42.   I. E. Yuzay, R. Auras and S. Selke, *Journal of applied polymer science*, 2010, **115**, 2262-2270.

43.   V. L. Finkenstadt, C.-K. Liu, R. Evangelista, L. Liu, S. C. Cermak, M. Hojilla-Evangelista and J. Willett, *Industrial Crops and Products*, 2007, **26**, 36-43.

44.   G. Yew, A. M. Yusof, Z. M. Ishak and U. Ishiaku, *Polymer Degradation and Stability*, 2005, **90**, 488-500.

45.   A. Gupta and S. Purwar, *Journal of applied polymer science*, 1985, **30**, 1799-1814.

46.   S. Maiti and R. Das, *International Journal of Polymeric Materials*, 2005, **54**, 467-482.

47.   N. Bitinis, R. Verdejo, P. Cassagnau and M. Lopez-Manchado, *Materials Chemistry and Physics*, 2011, **129**, 823-831.

48.   M. Kowalczyk, E. Piorkowska, S. Dutkiewicz and P. Sowinski, *European Polymer Journal*, 2014, **59**, 59-68.

49.   M. Evstatiev, S. Simeonova, K. Friedrich, X.-Q. Pei and P. Formanek, *Journal of Materials Science*, 2013, **48**, 6312-6330.

50.   L. Feng, X. Bian, Z. Chen, G. Li and X. Chen, *Polymer Degradation and Stability*, 2013, **98**, 1591-1600.

51.   Q. Zhao, Y. Ding, B. Yang, N. Ning and Q. Fu, *Polymer Testing*, 2013, **32**, 299-305.

52.   K. A. Afrifah and L. M. Matuana, *Macromolecular Materials and Engineering*, 2010, **295**, 802-811.

53.   Y. Li and H. Shimizu, *Macromolecular bioscience*, 2007, **7**, 921-928.

54.   S. Wu, *Journal of applied polymer science*, 1988, **35**, 549-561.

Graphical Abstract

Fabrication of Super Tough Poly(lactic acid)/Ethylene-*co*-vinyl-acetate Blends via Melt Recirculation Approach: Static-short term Mechanical and Morphological Interpretation
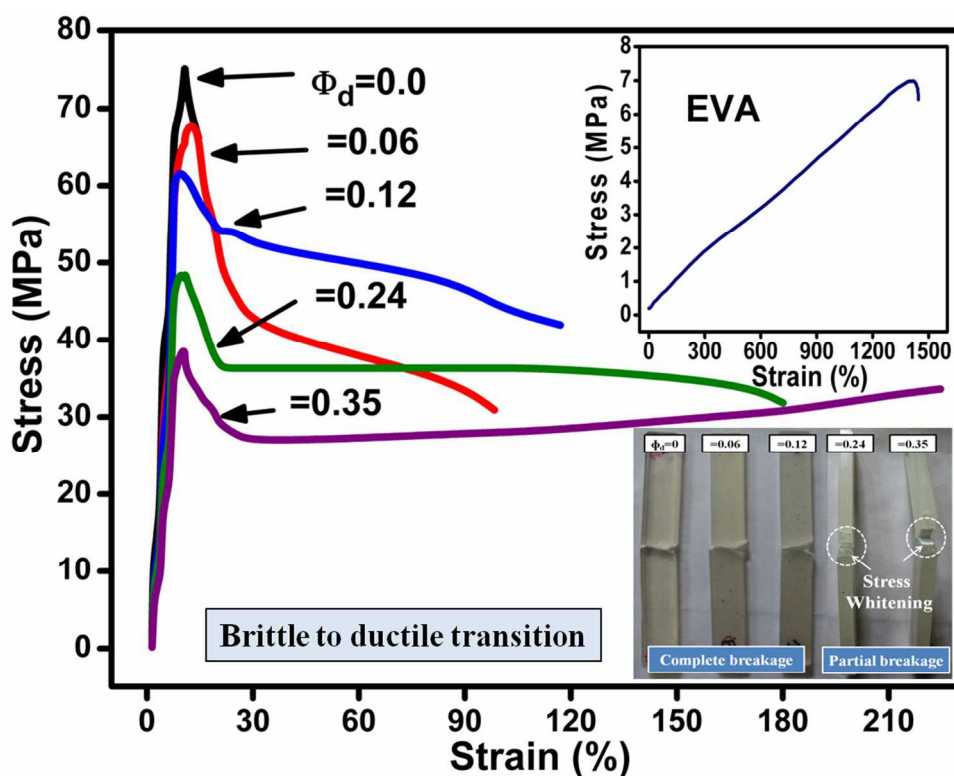
Rajendra Kumar, Saurindra N. Maiti[*], Anup K. Ghosh

Centre for Polymer Science and Engineering, Indian Institute of Technology Delhi,

Hauz Khas, New Delhi-110016, India

*Email address: maitisn49@yahoo.co.in

Tel.: +91-11-26591494; Fax: +91-11-26591421

The notched Izod impact strength of PLA/EVA blends enhanced significantly with improved toughness making blends super tough.